J Mater Sci (2007) 42:9030–9036
DOI 10.1007/s10853-007-1860-y

The effect of Sm substitution on properties of $Bi_{1.6}Pb_{0.4}Sr_2Ca_{2-x}Sm_xCu_3O_y$ superconductors

Mustafa Yilmazlar · Huseyin Aydin · Ahmet Varilci · Cabir Terzioglu

Received: 21 February 2007 / Accepted: 17 May 2007 / Published online: 20 July 2007

Abstract The effect of the partial substitution of Ca by Sm in the Bi-2223 superconducting samples have been investigated in terms of X-ray diffraction (XRD), EDXRF (Energy Dispersive X-ray Fluorescent), magnetoresistivity, critical temperature, transport critical current density, and ac susceptibility measurements. The samples were prepared by the conventional solid-state reaction method. XRD patterns are used to calculate lattice parameters and phase ratio of the Bi-2223 samples. The volume fraction was determined from the intensities of Bi-2223 and Bi-2212 peaks. The room temperature XRD patterns of the samples showed the presence of Bi-2223 phase decreases with increasing the Sm content. We estimated the transition temperature of the samples from the resistivity versus temperature measurements in dc magnetic fields up to 0.6 T. We observed that transition temperature, T_c, and transport critical current density, J_c^{trans}, depend on the Sm substitution. They both decrease with increasing the Sm substitution. We extracted the peak temperature, T_p, and the pinning force density from our previous ac susceptibility measurements. The pinning force density decreased with increasing the Sm content. The possible reasons for the observed decreases in critical temperature and critical current density due to Sm substitution were discussed.

M. Yilmazlar
Faculty of Education, Sakarya University, Sakarya, Hendek 54300, Turkey

H. Aydin · A. Varilci · C. Terzioglu (✉)
Department of Physics, Faculty of Arts and Sciences, Abant Izzet Baysal University, Bolu 14280, Turkey
e-mail: terzioglu_c@ibu.edu.tr

Introduction

It is understood that the high temperature superconductors (HTSCs) show unusual behaviors in the mixed state, smearing from their layered structure, high transition temperature, short coherence length and etc. Among these unusual behaviors, giant flux creep is suggested to be an important one, which has become an interesting subject for both theory and experiment in the past several years [1]. The results are used to discuss the flux pinning and thermally activated flux motion in the mixed state of HTSCs. These are related to the magnetic and electric properties of HTSCs in the magnetic field. The broadening of resistive transition in the magnetic field is also attributed to the thermally activated flux motion [2, 3]. Some groups [4–7] have done studies of flux pinning and flux activation, and several models have been proposed. Among these, both vortex-glass model [8] and collective-pinning model [9] predict the same power-law form for the dependence of the activation energy U_{eff} (J) on current density. According to the thermally activated flux motion model, the essential problem is to study the nonlinear U_{eff} (J) dependence of the HTSCs.

Magnetic relaxation and flux creep exists in type II superconductors causing decay of the irreversible magnetization. The irreversibility line can be determined from various measurements such as dc resistivity, ac susceptibility, and etc. [10]. Muller et al. [11] first reported the irreversibility line in HTSCs. The measurements of ac susceptibility are commonly used to determine magnetic and superconducting properties of materials. In particular, the ac susceptibility measurement is useful in determining the specimen and for distinguishing between inter- and intragrain properties. For sintered high-T_c superconductors the temperature dependence of the imaginary part of the

complex ac susceptibility shows two peaks, T_p and T_g, at high ac fields [12, 13]. The first peak (at high field) appears at a temperature T_g slightly bellow T_c due to intragranular supercurrents, and a second loss peak (at low-field) appears at a temperature T_p lower than T_g due to sample-circulating intergranular supercurrents.

Doping with different elements at various amounts and adjusting preparation condition affect phase formation and physical properties in Bi-based system. Many studies of doping into superconductor oxide ceramics have been made in order to improve their superconducting, magnetic and mechanical properties [14–21]. The objectives of doping studies are to optimize the hole concentration, to introduce pinning centers and to enhance the formation of Bi-2223 phase. Li, Ti, W and Mo have been doped into BiPbSrCaCuO bulk samples, and it was reported that Li doping led to an increase in critical current density (J_c), while Ti doping led to a decrease, and W and Mo doping did not contribute a substantial change in J_c [23, 24]. Substitution of Eu, Dy and Tm in the Bi-2212 system has caused a transition from superconductor to insulator [24–26]. The partial replacements of Ca by Y, Gd, and Sm in the Bi-2212 and Bi-2223 systems decreased carrier concentration due to structural modulations and changes in the valency of Cu [25–28]. On the other hand, it was observed that the substitution of divalent Ca by trivalent rare-earth elements in the Bi-2212 system causes a sharp change in transition from a superconductor to an insulator and a decrease in the lattice parameter c because of a drastic change in the carrier concentration [22, 27]. A comprehensive study of Sm addition to Bi-2212 and Bi-2223 was reported in the literature [16–19, 29]. In our previous study, we investigated the effect of the partial substitution of Ca by Sm in the Bi-2223 superconducting samples on its structural and physical and magnetic properties [16–19]. It was obtained that superconducting (the values of T_c and J_c) and mechanical properties degrade and the lattice parameter c and the Bi-2223 phase decreased with increasing Sm content. It was also reported that for $x = 1.0$ and 1.5 the compounds showed semiconducting behavior. We investigated effect of the partial substitution of Ca by Sm in Bi(Pb)SrCaCuO system by using the low field ac magnetic susceptibility method [18]. The investigations consisted of ac susceptibility, the temperature dependence of intergranular critical current density, $J_c^{inter}(T_p)$, and scanning electron microscopy (SEM) measurements. It was observed that the grain size of the pure sample is considerably larger than the Sm-doped samples, the overall susceptibility curves of the samples are shifted to lower temperature and the value of $J_c^{inter}(T_p)$ decreases by increasing the Sm concentration.

In this work, we report measurements of electrical resistivity as a function of temperature under magnetic field up to 0.6 T and transport critical current density in order to investigate the effect of the partial substitution of Ca by Sm on superconducting properties of Bi-2223 samples. We also reported XRD measurements to extract the lattice parameters and the relative portion of Bi-2223 and that of Bi-2212 phases and EDXRF measurements to estimate stoichiometric ratios of the considered samples.

Experimental details

The $Bi_{1.6}Pb_{0.4}Sr_2(Ca_{2-x}Sm_x)Cu_3O_y$ samples with $0 < x < 0.005$ Sm were prepared by using the standard solid-state reaction method [16]. Rectangular bars were cut from the sintered samples for electrical resistivity, critical current and ac susceptibility measurements. The typical sample size was $2.9 \times 2.1 \times 12.1$ mm^3.

XRD data were taken using a Rigaku D/Max-IIIC diffractometer with CuK_α radiation in the range $2\theta = 4°$–$60°$ with a scan speed of 3°/min and a step increment of 0.02° at room temperature. Phase purity and the lattice parameters were obtained from these XRD patterns. The accuracy in determining the lattice parameter c was ±0.001 Å. The mean values of lattice parameter c for Bi-2223 phase are determined from (002), (00$\underline{1}$0), (00$\underline{1}$2), (115) and (00$\underline{1}$4) peaks of the XRD measurements for pure and Sm substituted $Bi_{1.6}Pb_{0.4}Sr_2(Ca_{2-x}Sm_x)Cu_3O_y$ samples. The relative proportions of the Bi-2223 phase were determined from (002), (008), (00$\underline{1}$0), (115), (00$\underline{1}$2), (200), (11$\underline{1}$1) and (02$\underline{1}$2) peaks and the relative proportions of Bi-2212 phase were determined from (115), (220), (315), (317), (11$\underline{1}$5) and (11$\underline{1}$2) peaks. The relative proportions of the Bi-2223 phase were determined from (002), (008), (00$\underline{1}$0), (115), (00$\underline{1}$2), (200), (11$\underline{1}$1) and (02$\underline{1}$2) peaks and the relative proportions of Bi-2212 phase were determined from (115), (220), (315), (317), (11$\underline{1}$5) and (11$\underline{1}$2) peaks, using the following well-known expressions [30, 31];

$$f_{(2223)} = \frac{\sum I_{H(hkl)}}{\sum I_{H(hkl)} + \sum I_{L(hkl)}} \quad (1)$$

$$f_{(2212)} = \frac{\sum I_{L(hkl)}}{\sum I_{H(hkl)} + \sum I_{L(hkl)}} . \quad (2)$$

Here I_H(hkl) and I_L(hkl) are the intensities of the (hkl) diffraction lines for Bi-2223 and Bi-2212 phases, respectively (Fig. 2).

The transport critical current (I_c) (77 K, self field, 1 μV cm^{-1}) and dc resistivity (5 mA dc current) were measured by a conventional four-probe method. The contacts were made with silver paint. The outside pin-points feed the current and the intermediate ones ($l = 7$ mm) allow the voltage drop measurement. A Keithley 220

programmable current source and a Keithley 2182A nanovoltmeter were used for the resistivity and I–V measurements. The I_c was converted to J_c^{trans} by dividing by the area of cross section of the samples. Actual dc currents were run through the samples up to 5 A. Resistive contacts caused heating and the test was completed in possible short time, in order to avoid this effect.

We measured temperature (40–130 K) and dc magnetic field (0–0.6 T) dependent of resistivity of the samples with 5 mA dc current in a cryostat. The magnetic field was applied parallel to the current direction. The external dc magnetic fields for resistivity measurements were provided by an electromagnet. The transition temperature T_c was determined as the temperature at zero resistivity.

Results and discussion

In our previous work, we investigated effect of the partial substitution of Ca by Sm in Bi(Pb)SrCaCuO high temperature superconductors by using the low field ac magnetic susceptibility method [18]. The investigations consisted of ac susceptibility as a function of temperature (77–120 K) under different ac field amplitudes, the temperature dependence of intergranular critical current density, $J_c^{inter}(T_p)$, and SEM measurements. It was observed that the overall susceptibility curves of the samples are shifted to lower temperature by increasing the ac field amplitude. The intensity of the imaginary parts increased with increasing the ac field amplitude. The susceptibility–temperature curves shifted to lower temperatures and considerably increased the transition width in $\chi'' - T$ curves, and also decreased the shielding fraction of the superconducting phase in the samples with increasing the Sm concentration. In the calculation of $J_c^{inter}(T_p)$ as a function of the peak temperature from our previous work [18], it was found that the value of $J_c^{inter}(T_p)$ increases with decreasing the Sm content and temperature. From the previous SEM analysis [16], it was observed that the grain size of the pure sample is considerably larger than the Sm-doped samples.

In the present study, we have studied the peak temperature dependence as a function of ac magnetic field, H_{ac}, in order to investigate the effect of partial substitution of Ca by Sm on the intergranular pinning force. The values of T_p were estimated from our previous ac susceptibility versus temperature measurements for the ac field amplitudes of 111, 222, 333, 444 and 555 A/m at 1 kHz [18]. It was also observed that peak temperatures, T_p, shift to lower temperature with increasing ac field amplitudes. The shift of T_p with field can be explained in terms of the strength of the pinning force. As can be seen from Fig. 1 a linear dependence of T_p as a function of H_{ac} is observed for all the

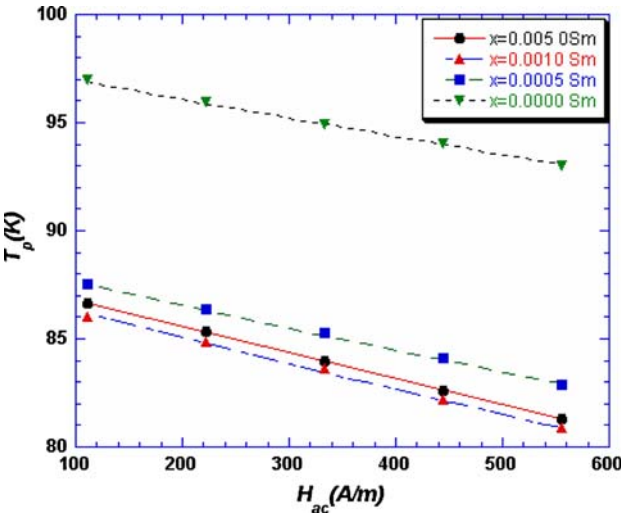

Fig. 1 Intergranular peak temperature as a function of ac magnetic field amplitude for x = 0.0000, 0.0005, 0.0010, and 0.0050 Sm

samples. This is consistent with the previous works [32–34]. Müller critical state model assumes a magnetic flux independent pinning force densities, and α_J and α_g for inter- and intragranular vortices described by the relation [33]:

$$T_p = T_{p0} - T_{p0}\left[\frac{\mu_0 \mu_{eff}(0)}{2a\alpha_J(0)}\right]^{1/2} H_{ac} \tag{3}$$

where a is the height of the cylinder samples, $\mu_{eff}(0)$ is the effective permeability of the ceramic and α_J (0) is the intergranular pinning force density. From a least squares fit of this expression (Eq. (3)) to the data T_{p0} and $\left[\mu_0 \mu_{eff}(0)/2a\alpha_J(0)\right]$ were extracted for all samples. The values of T_{p0} decreased while the values of $\left[\mu_0 \mu_{eff}(0)/2a\alpha_J(0)\right]$ increased with increasing the Sm content. This means that the values of α_J (0) decrease with increasing the Sm concentration. A decreasing trend in pinning force of the samples with increasing the Sm content is attributable to greater voids and defects as revealed by our previous SEM images [16]. This result is also consistent with the temperature dependence of $J_c^{inter}(T_p)$ in the previous study [18]. The effective pinning force density decreases with increasing ac magnetic field causing T_p to shift to lower temperature. The rapid decrease of the activation energy induces the steep dropping of the critical current density with increasing magnetic field.

The XRD patterns of pure and Sm substituted samples (x = 0, 0.0005, 0.001 and 0.005) are shown in Fig. 2. XRD pattern was taken by use of CuK_α radiation and measurements were taken at room temperature. All peaks in the XRD pattern are indexed. There is a significant increase in the intensities of particular peaks between the pure and Sm substituted samples. As can be seen from the figure, the intensities of the Bi-2223 peaks decrease and the intensities

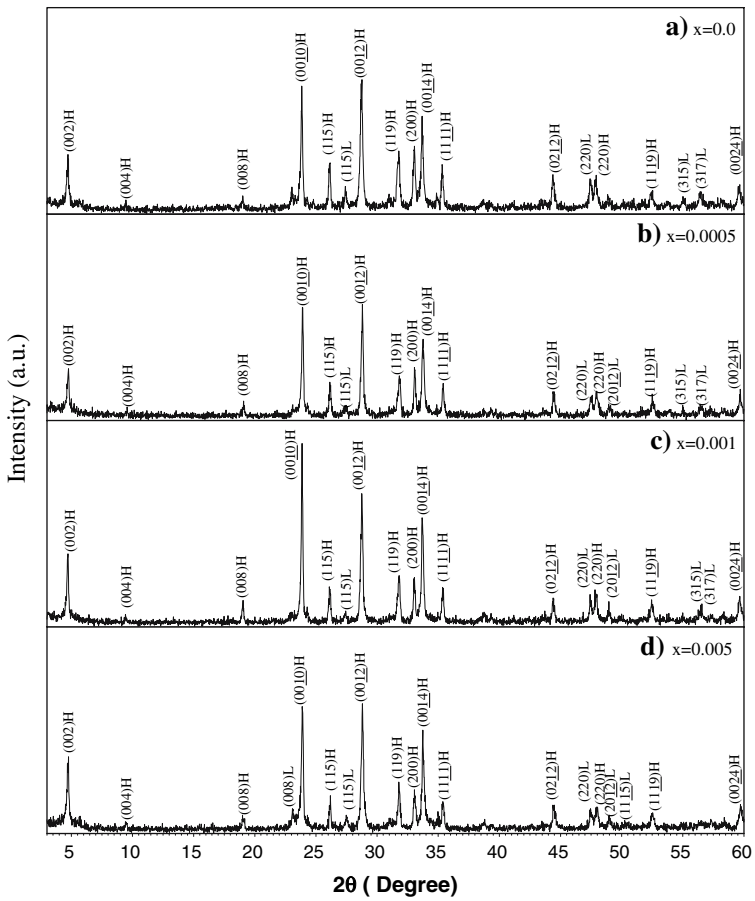

Fig. 2 The XRD patterns for (**a**) pure sample and Sm substituted samples (**b**) x = 0.0005, (**c**) 0.001, and (**d**) 0.005. The peaks indexed (*hkl*)L and (*hkl*)H represent the Bi-2212 and Bi-2223 phases, respectively

of the Bi-2212 peaks increase with increasing substitution of Sm for Ca. The determined lattice parameters from the (00*l*) peaks of the XRD data are given in Table 1. It is observed that the lattice parameter *c* decreases significantly with increasing *Sm* content as listed in Table 1. Similar result has been reported by Zandbergen et al. [35]. As pointed out by Zandbergen et al., the behavior of lattice parameter can be explained by the increase of the oxygen content in the unit cell by the replacement of Ca^{2+} by Sm^{3+} in the structure. It was speculated that the excess of oxygen goes into the bismuth oxide layers causing a decrease in lattice parameter *c*. It is also believed that the decrease of lattice parameter *c* is due to incorporation of Sm ions into the interstitial sites in the unit cell rather than occupation of the Ca sites. The relative volume fractions of the Bi-2223 and Bi-2212 phases were determined from the peak intensities of the same particular reflections using Eqs. (1) and (2). As listed in Table 1, the volume fraction of Bi-2223 phase decreased and that of Bi-2212 phase increased with increasing the Sm content.

Table 1 Some characteristics of superconducting samples

Samples	Lattice parameter *c* (Å)	Volume fraction (%)		T_c^{onset} (K)	T_p (K) (for 111 A/m)
		Bi-2223	Bi-2212		
Pure	37.236	94	06	105	97
x = 0.0005	37.206	92	08	102	88
x = 0.001	37.197	83	17	99	86
x = 0.005	37.190	79	21	97	85

The stoichiometry of Sm substituted annealed $Bi_{1.6}Pb_{0.4}Sr_2Ca_{2-x}Sm_xCu_3O_y$ samples were investigated by EDXRF technique. Figure 3 shows the EDXRF spectrum of Sm substituted $Bi_{1.6}Pb_{0.4}Sr_2Ca_{2-x}Sm_xCu_3O_y$ samples with x = 0.0005, 0.001 and 0.005. Stoichiometric ratios of the analysed samples are given in Table 2 [19]. In this analysis, Bi atomic ratio is given as 1.6. As seen from the table, Sm amount in the sample up to x = 0.001 is not enough to examine by means of the EDXRF technique.

The electrical resistivity as a function of temperature was measured in an external magnetic field up to 0.6 T for the $Bi_{1.6}Pb_{0.4}Sr_2(Ca_{2-x}Sm_x)Cu_3O_y$ samples with $0 < x < 0.005$ Sm. Figure 4 shows temperature dependence of resistivity for $Bi_{1.6}Pb_{0.4}Sr_2(Ca_{2-x}Sm_x)Cu_3O_y$ with x = 0, 0.0005, 0.0010 and 0.0050 at zero fields. The resistivity versus temperature plots show that the resistivity

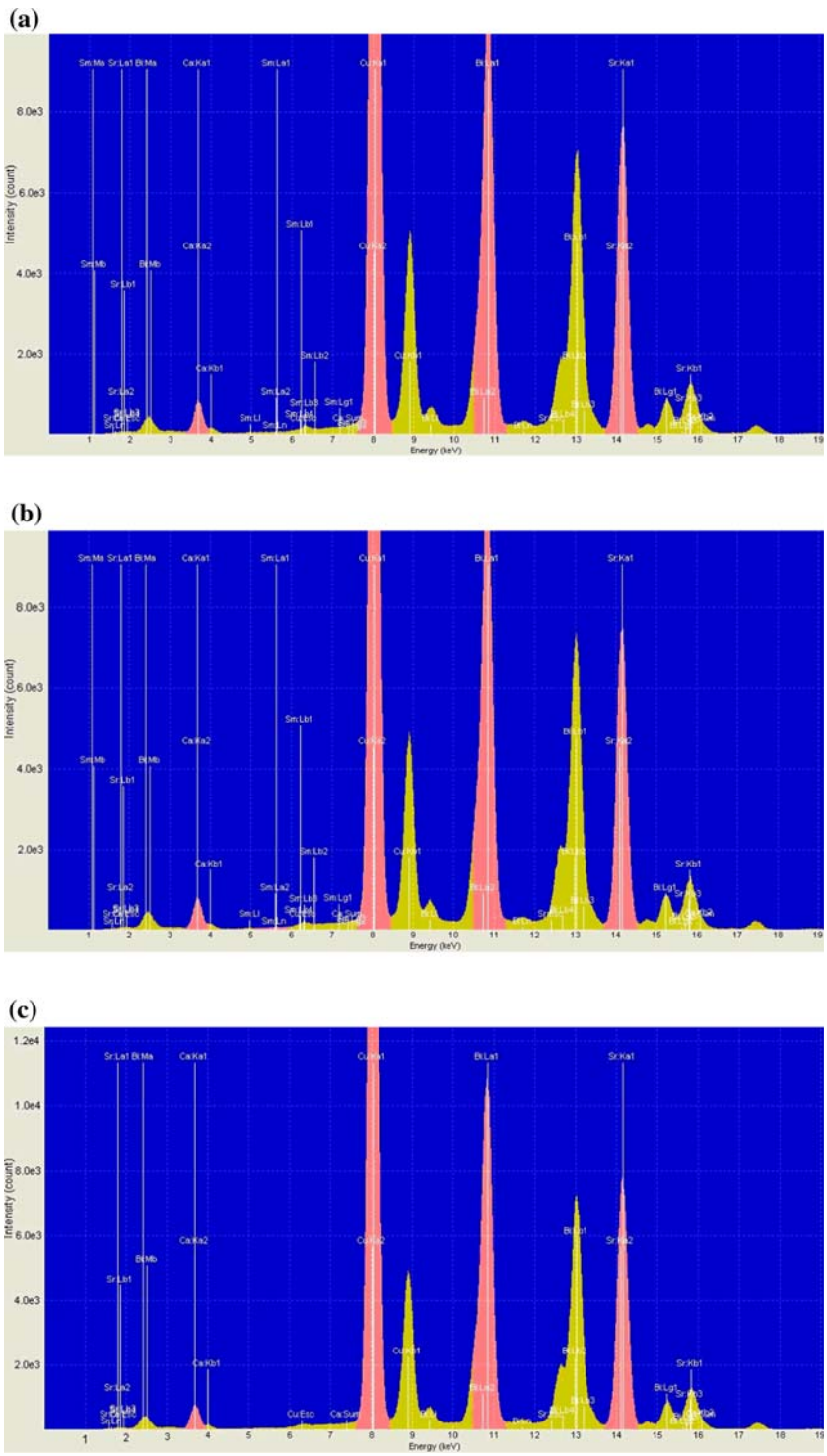

Fig. 3 EDXRF spectra of $Bi_{1.6}Pb_{0.4}Sr_2Ca_{2-x}Sm_xCu_3O_y$ samples with (**a**) $x = 0.0005$, (**b**) $x = 0.001$ and (**c**) $x = 0.005$

decreases linearly with temperature in the normal state. As can be seen from the figure the transition temperature, T_c^{offset}, decreases from 90 K to 75 K with increasing the Sm concentration at zero magnetic field. Room temperature resistivity increases while critical transition temperature decreases with increasing x from zero to 0.005 Sm. The behavior of the resistivity is the same as our previous measurements [16] except the values of transition temperature and room temperature resistivity. In the present work, dc resistivity measurements on the same samples were made approximately 2 years later than the previous work. It is observed that the values of T_c decrease while the values of room temperature resistivity increase (10 times) in the present study. The transition curves from normal to

Table 2 Calculated stoichiometry of Sm substituted $Bi_{1.6}Pb_{0.4}Sr_2Ca_{2-x}Sm_xCu_3O_y$ samples from EDXRF results [19]

Samples	Bi	Sr	Ca	Sm	Cu
Pure	1.600	0.950	0.320	0.003	1.790
$x = 0.0005$	1.600	0.860	0.240	0.000	1.730
$x = 0.0010$	1.600	0.850	0.240	0.000	1.760
$x = 0.0050$	1.600	0.820	0.2300	0.005	1.680
$x = 0.0100$	1.600	0.800	0.220	0.007	1.580
$x = 0.1000$	1.600	0.820	0.200	0.063	1.650

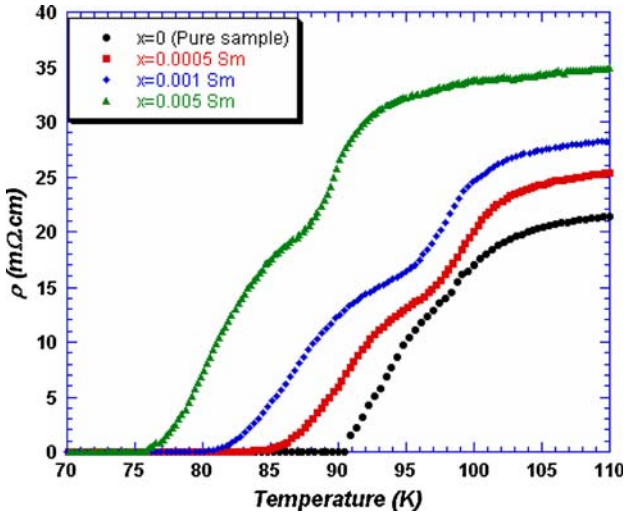

Fig. 4 Temperature dependence of resistivity for $Bi_{1.6}Pb_{0.4}Sr_2(Ca_{2-x}Sm_x)Cu_3O_y$ with $x = 0$, 0.0005, 0.001 and 0.005 at zero fields

superconducting state indicate two-step transitions and it is believed that it is related to a structural phase transformation (from 2223 to 2212) and weak links between the grains in the samples. The structural phase transformation is supported by XRD measurements. It is observed that the broadening of the resistivity transition width increases with increasing the Sm concentration.

Figure 5 shows temperature dependence of resistivity for $Bi_{1.6}Pb_{0.4}Sr_2(Ca_{2-x}Sm_x)Cu_3O_y$ with $x = 0.0005$ and $x = 0.001$ at various magnetic fields (0, 0.3 and 0.6 T). It is observed that, with increasing dc magnetic field up to 0.6 T, T_c^{offset} ranges from 90 K to 70 K for the pure sample, 85 K to 54 K for $x = 0.0005$ Sm, 80 K to 49 K for $x = 0.001$ Sm, and 75 K to 35 K for $x = 0.005$ Sm.

The transport critical current densities as a function of the Sm concentrations were measured in liquid nitrogen at zero magnetic fields as shown in Fig. 6. It observed that the J_c^{trans} decreases with increasing the Sm concentrations. This result agrees with our $\alpha_J(0)$ calculations. Granularity of the samples was the reason for low critical current densities. The relatively low J_c^{trans} for Sm substituted sample with respect to the undoped sample may be attributed to have smaller grain size.

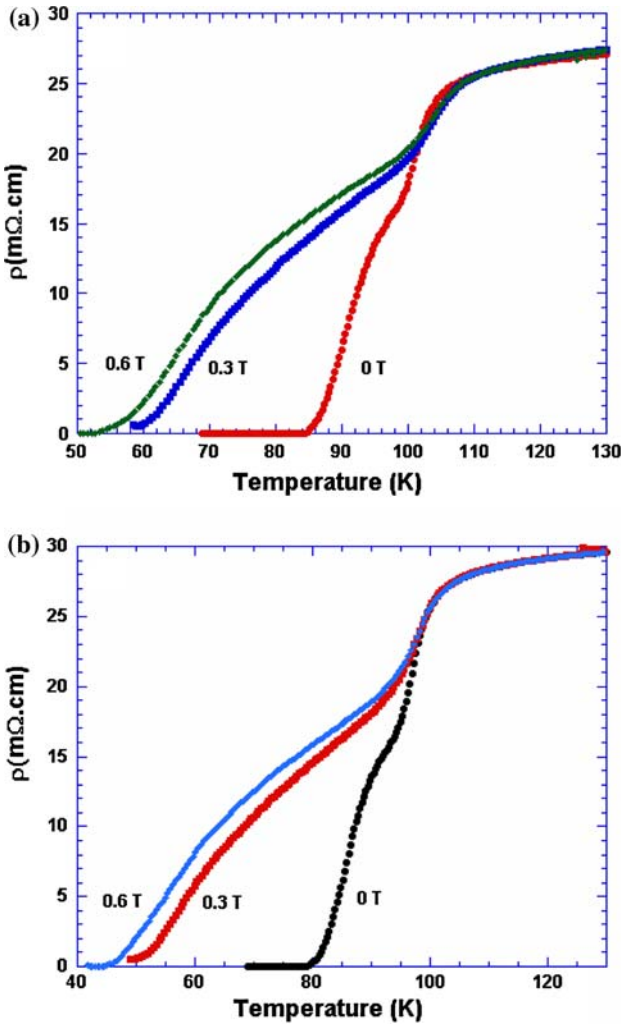

Fig. 5 Temperature dependence of resistivity for $Bi_{1.6}Pb_{0.4}Sr_2(Ca_{2-x}Sm_x)Cu_3O_y$ with (**a**) $x = 0.0005$ and (**b**) $x = 0.0010$ at various magnetic fields

Conclusions

Superconducting samples with nominal composition $Bi_{1.6}Pb_{0.4}Sr_2(Ca_{2-x}Sm_x)Cu_3O_y$ were prepared the solid-state reaction method. The XRD measurements were done at room temperature and the lattice parameters of the samples were obtained by indexing all the peaks. The

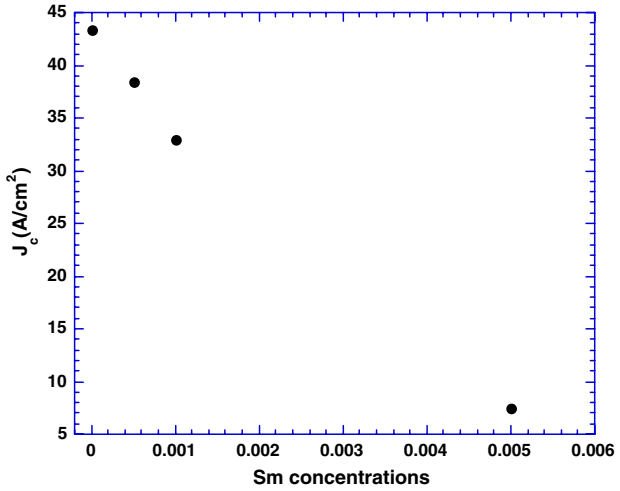

Fig. 6 Transport critical current density versus Sm concentration at 77 K

measurements show that there exist two phases for all the samples in which Bi-2223 phase decreases while Bi-2212 phase increases with increasing the Sm content. The dc electrical resistivity and critical current density measurements were carried out on the samples. The Sm → Ca substitution in $Bi_{1.6}Pb_{0.4}Sr_2(Ca_{2-x}Sm_x)Cu_3O_y$ system decreased the J_c^{trans} and T_c of the samples. T_c^{onset} ranged from 102 K to 98 K for the pure and the Sm-doped samples, respectively. The temperature dependence of the electrical resistivity is linear in the normal state. Room temperature resistivity increases with increasing x from zero to 0.005 Sm. The width of intragrain transition increases with increasing the Sm content and external dc magnetic field. It is observed that T_c, and J_c^{trans} depend on both the Sm content of samples and the applied magnetic field. The calculated α_J (0) from our previous ac susceptibility measurements, we found that the values of α_J (0) decrease with increasing the Sm concentration.

Acknowledgments This work is supported partly by Research Foundation of Kirikkale Univerity (Project No: 2005/39), partly by The Scientific and Technological Council of Turkey (Project No: 104T325) and partly by SRP unit of Abant Izzet Baysal University (Project No: 2003.03.02.194).

References

1. Sun JJ, Zhao BR, Li L, Xu B, Li JV, Guo SQ, Yin B (1997) Physica C 291:257
2. Tinkham M (1988) Phys Rev Lett 61:1658
3. Palstra TTM, Batlogg B, Schneemeyer LF, Waszczak JV (1988) Phys Rev Lett 61:1662
4. Anderson PW (1962) Phys Rev Lett 9:309
5. Beasley MR, Labusch R, Webb WW (1969) Phys Rev 181:682
6. Maley MP, Wills JO, Lessure H, McHenry ME (1990) Phys Rev B 42:2639
7. Zeldov E, Amer NM, Koren G, Gupta A, McElfresh MW, Kambino RJ (1990) Appl Phys Lett 56:680
8. Fisher MPA (1989) Phys Rev Lett 62:1415
9. Feigel'man MV, Geshkenbein VB, Larkin AI, Vinokur VM (1989) Phys Rev Lett 63:2303
10. Nezir S, Celebi S, Altunbas M (2000) J Alloys Compd 302:235
11. Muller KH, Takashige M, Bednorz JG (1987) Phys Rev Lett 58:1143
12. Clim JR (1991) Physica C 50:153
13. Muller KH, Macfarlane JC, Driver R (1988) Physica C 203: 178
14. Pan SH, Hudson EW, Lang KM, Eisaki H, Uehida S, Davis JC (2000) Nature 403:746
15. Eisaki H, Kaneko N, Feng DL, Damascelli A, Mank PK, Shen KM, Shen ZX, Greven M (2004) Phys Rev B 69:064512
16. Terzioglu C, Yilmazlar M, Ozturk O, Yanmaz E (2005) Physica C 423:119
17. Yilmazlar M, Cetinkara HA, Nursoy M, Ozturk O, Terzioglu C (2006) Physica C 442:101
18. Terzioglu C, Yegen D, Yilmazlar M, Görür O, Akdoğan M, Varilci A (in press) J Mater Sci, doi: 10.1007/s10853-006-0541-6
19. Yegen D, Varilci A, Yilmazlar M, Terzioglu C, Belenli I (in press) Physica C
20. Prabitha VG, Biju A, Abhilash Kumar RG, Sarun PM, Aloysius RP, Syamaprasad U (2005) Physica C 433:28
21. Nanda KK, Muralidhar M, Hari Babu V, Pena O, Sergent M, Beniere F (1993) Physica C 229–304:204
22. Awana VPS, Agarwal SK, Ray R, Gupta S, Narlikar AV (1992) Physica C 191:43
23. Kambe S, Guo YC, Dou SX, Liu HK, Wakahara Y, Maeda H, Kakimoto K, Yavuz M (1998) Supercond Sci Technol 11:1061
24. Kambe S, Guo YC, Dou SX, Liu HK (1996) Proc R Soc London 96:454
25. Kishore KN, Satyavathi S, Muralidhar M, Babu VH, Pena O, Sergent M, Beniere F (1994) Phys Status Solidi A 143:101
26. Kishore KN, Satyavathi S, Babu VH, Pena O (1996) Mater Sci Eng B38:267
27. Kishore KN, Muralidhar M, Babu VH (1993) Physica C 204:299
28. Satyavathi S, \Muralidhar M, Kishore KN, Babu VH (1995) Appl Superconductivity 3:187
29. Prabitha VG, Biju A, Abhilash Kumar RG, Sarun PM, Aloysius RP, Syamaprasad U (2005) Physica C 433:28
30. Chiu CW, Meng RL, Gao L, Huang ZJ, Chen F, Xue YY (1993) Nature 365:323
31. Halim SA, Khawaldeh SA, Mohammed SB, Azhan H (1999) Mater Chem Phys 61:251
32. Ilonca G, Pop AV, Yang T-R, Jurcut T, Lung C, Stiufiuc G, Stiufiuc R, Panfilescu IA (2001) Int J Inorg Mater 3:763
33. Babic E, Drobac D, Horvat J, Marohnic Z, Prester M (1989) J Less Comm Met 151:89
34. Ozturk O, Yegen D, Yilmazlar M, Varilci A, Terzioglu C (2007) Physica C 451:113
35. Zandbergen HW, Greon WA, Smit A, Tendeloo GV (1990) Physica C 168:426